Theoretical and Experimental Investigations of Polyelectrolyte Adsorption Dependence on Molecular Weight

Xie, Fei; Lu, Hongduo; Nylander, Tommy; Wågberg, Lars; Forsman, Jan

Published in:
Langmuir

DOI:
10.1021/acs.langmuir.6b00668

2016

Theoretical and experimental investigations of polyelectrolyte adsorption dependence on molecular weight

Fei Xie*, Hongduo Lu*, Tommy Nylander**, Lars Wågberg*** and Jan Forsman*

*Theoretical Chemistry, Lund University, P.O.Box 124, S-221 00 Lund, Sweden

**Physical Chemistry, Lund University, P.O.Box 124, S-221 00 Lund, Sweden

***Wallenberg Wood Science Center, KTH Royal Institute of Technology, S-100 44 Stockholm, Sweden

E-mail: fei.xie@teokem.lu.se

Abstract

This work focuses on adsorption of polyions onto oppositely charged surfaces, and responses to the addition of simple monovalent salt as well as polyion length (degree of polymerization). We also discuss possible mechanisms underlying observed differences, of the adsorbed amount on silica surfaces at high pH, between seemingly similar polyions. This involves theoretical modelling, utilizing classical polymer density functional theory. We furthermore investigate how long and short chain versions of the polymer adsorb onto carboxymethylated cellulose, carrying a high negative charge. Interestingly enough, comparing results obtained for the two different surfaces, we observe an opposite qualitative response on molecular weight. The large polymer adsorb more strongly at a silica surface, but for cellulose at low salt levels, there are indications that the trend is opposite. Another difference is the very slow

*To whom correspondence should be addressed

adsorption process observed to cellulose, particularly with short polymers; in fact with short polymers we were sometimes unable to establish any adsorption plateau at all. We speculate that the slow dynamics is due to a gradual diffusion of short polymers into the cellulose matrix. This phenomenon could also explain why short chain polymer seems to adsorb more strongly than long ones, at low salt concentrations, provided that the latter then are too large to enter the cellulose pores. Cellulose swelling at high salt might diminish these differences, leading to more similar adsorbed amounts, or even a lower adsorption for short chains.

Introduction

The adsorption of charged polymers onto oppositely charged surfaces has been rather extensively studied in the past.[1–29] However, due to detection limitations, most studies have been devoted to polymers that carry a relatively low linear charge density, or those that contain titrating groups. The reason is that these polymers tend to adsorb at least strongly enough to neutralize the surface charge. The use of modestly charged chains will ensure a large adsorbed mass, which is easier to measure. Nevertheless, highly charged polymers are of course still relevant. They can be expected to adsorb very strongly, quite possibly to an extent that overcompensates the bare surface charge. This also has relevance to the interaction between charged surfaces or particles, since such an overcharging may lead to a long ranged double layer repulsion, and a concomitant free energy barrier against flocculation.

This work is composed of two parts. In the first, we extend our earlier study of the adsorption of highly charged non-titrating cationic polymers onto a highly charged silica surface, at pH 9. Specifically, we will compare the adsorption of long and short chains of Poly(4-vinyl N-methylpyridinium iodide), PVNP, with particular focus on how this is affected by the concentration of simple monovalent salt. The results from these measurements will be interpreted and discussed via theoretical analyses, based on *classical* (statistical-mechanical) polymer density functional theory, DFT. We will extend our previous treatment, and compare predictions with those obtained from a slightly different model. This will allow us to scrutinize possible ori-

gins for the observed differences between the adsorption of PVNP and the (similarly charged) Poly(diallyldimethylammonium chloride), PDADMAC. The second part of our work is devoted to a similar analysis on salt dependent adsorption of high and low molecular weight PVNP. The surface is here composed of carboxymethylated cellulose, which carries a high negative charge in aqueous solution, at pH 9.

Before we present our work, it is appropriate to review results from related studies in this area. Hierrezuelo *et al.*[23] used dynamic light scattering to study the thickness of PDADMAC and linear PEI layers on oppositely charged sulfate latex particles. The measured thicknesses were almost independent of salt concentration at low levels of salt, but increased substantially at higher concentrations. In a related study, Seyrek *et al.*[25] used the same technique to investigate the dependence of layer thickness on polymer molecular weight. They observed an increase with polymer length at high salt levels, but only a weak dependence at low ionic strengths. M*észá*ros et al.[11,30] studied how the adsorption of branched PEI on silica varies with pH, at low salt. The adsorption was found to increase with salt, at a given pH, and to increase with pH, at a given salt concentration. It should be noted that PEI as well as silica are expected to titrate in the investigated interval. Shubin and Linse[7] investigated the adsorption of weakly charged polyacrylamide on oppositely charged silica, using ellipsometry. According to their results, the adsorbed amount is constant at low salt concentrations, and decreases with ionic strength at high levels. Liufu *et al.*[31] investigated the adsorption of MPTMAC on silica nanoparticles in aqueous solution, and observed an adsorbed amount displaying a maximum as a function of salt concentration. Enarsson *et al.*[20] and Saarinen *et al.*[21] also observed this behaviour, when they studied the adsorption of CPAM on cellulose fibers and silica surfaces. Qualitatively similar findings were noted by Hansupalak *et al.*,[12] who measured the adsorbed amount of DMAEMA on silica, as a function of ionic strength at various pH values. Guzm*á*n et al.,[27] on the other hand, observed a monotonically increasing adsorbed amount, as salt was added. Rojas[32] *et al.* found that the adsorption of rather weakly cationic polymer on mica decreased monotonically with salt concentration. Finally, we mention that Guzm*á*n et al.[22] investigated how adsorption equilibrium and adsorption kinetics depend upon

polymer nature as well as on the surface charge density.

We believe that one important reason for the lack of qualitative agreement between some of the experimental works mentioned above, is that many of them have focused on weakly charged polymers. As already pointed out, this is convenient from a mass detection point of view, but the importance of purely *electrostatic* effects may then not dominate the observed behaviours. In those cases, it is of course possible that the addition of salt can lead to a range of different responses, including virtually no response. In this work, we shall continue our previous efforts to emphasize effects from electrostatic interactions. This is achieved by working with highly charged, and non-titrating, polymers and surfaces carrying a strong but opposite charge. Specifically, we will here focus on polymer length effects, as studied with two very different surfaces, both of which are negatively charged. As we shall see, the composition and structure of the surface can even qualitatively influence the response of adsorption to changes of the polymer length.

Experimental section

Materials

Polyelectrolyte solutions

Highly charged polyelectrolytes, poly(4-vinyl N-methylpyridinium iodide) (PVNP), purchased from Polymer Source Inc. Quebec H9P 2X8, Canada, with two different molecular weights, 64.8 kg/mol and 4.6 kg/mol respectively, were used in this work to investigate the polymer adsorption. The chemical structure of PVNP is shown in Figure 1. According to the supplier, the reported average degree of polymerization (number averaged, M_n) for the long chain PVNP is 220, while for the short chain is 16. The polydispersity index (PDI) is 1.2 and 1.15 for the long and short chain, respectively (supplier data).

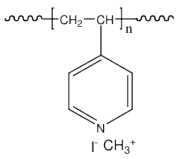

Figure 1: Chemical structure of PVNP.

PVNP is a water-soluble polyelectrolyte. The powder was dissolved into different concentrations of NaCl solution, adding 1mM Tris(Hydroxymethyl) aminomethane (Tris) buffer in order to keep the pH close to 9. The solution was filtrated by using a 0.22 μm syringe filter. The target monomer concentration of the PVNP stock solution is 2 mM. The stock solution was diluted 10-fold (to 0.2 mM) when injected into the measuring cell of the ellipsometer.

Silica substrate

Silicon wafers were purchased from Semiconductor Wafer, Inc. (NO.3) Taiwan, with one side polished, and p-doped with boron. The thermal oxide layer (SiO_2 layer) thickness of the silica wafer was around 30 nm. The silica wafers were cut into rectangular pieces: 1cm $\times$ 3cm which are suitable dimensions for the sample holder of the ellipsometer. The substrates were cleaned by immersion in a mixture of Milli-Q water, NH_3, and H_2O_2 at 80 °C for 5 min, followed by a mixture of Milli-Q water, HCl and H_2O_2 at 80 °C for 10 min. Finally, the substrates were rinsed with Milli-Q water and ethanol. The slides were immersed into 1mM NaOH solution for 40 min prior to ellipsometry measurements. A plasma cleaner (model PDC-3XG, Harrick Scientific Corp.) was used as a final cleaning step. The slides were kept in the plasma cleaner for 5 min, with the residual air adjusted to 0.03 mbar, and the power consumption was set to 30W.

Cellulose surfaces

Negatively charged (at pH 9) carboxymethylated cellulose fibers (350 μeq/g) were used in this study to produce cellulose surfaces. The method of making a cellulose coated surface on a silica substrate has been detailed in earlier work.[33,34] 0.25g carboxymethylated cellulose fiber was

dissolved into 12.5g 4-Methylmorpholin N-Oxide (NMMO) Solution (Sigma Aldrich, 50% wt). 37.5g Dimethyl sulfoxide (DMSO, Sigma Aldrich) was subsequently added, in order to dilute the viscous cellulose solution, since cellulose precipitate slowly in DMSO. The solubilisation was promoted by stirring the solution at 125 °C for 1h. The solution then became clear, with an orange colour, indicating that the cellulose had dissolved completely. The solution was then left at room temperature for around 40 min, in order to cool down.

The silica substrate, was cleaned with a plasma cleaner for 2 min, and then immersed into 7 wt % cationic poly(vinylamine) polyelectrolyte (PVAm; Lupamin 9095) solution for 15 min, and Milli-Q water for 15 min, then dried by nitrogen gas gently, in order to deposit a cationic polymer layer on the surface, which acts as a "glue" between the negatively charged silica surface and the cellulose fiber.

A spin-coater (model LabSpin, SÜSS MicroTec AG, Germany) was used to produce cellulose coated surfaces on silica slides. A silica slide was mounted in the spin-coater and a droplet of cellulose solution (around 100 μl) was applied on the surface, followed by spinning at 1500 rpm for 15s and 3500 rpm for 30s, in order to spread the cellulose evenly on the substrate. The cellulose coated surface was then immersed into Milli-Q water for 1h, follwed by drying with nitrogen. This procedure generates a uniform cellulose coated surfaces, with a cellulose thickness of around 30 nm.

The prepared cellulose substrates were stored in a desiccator, and then immersed in a salt solution for around 1h prior to the ellipsometry measurements, in order to let the cellulose layer fully swell. This procedure resultet in stable optical properties of the cellulose layer, as monitored by the ellipsometer readings.

Methods

An Abbe refractometer (Abbe 60/ED) was used to measure the refractive index increment (dn/dc) for the polyelectrolytes, as well as the refractive index of salt solutions at various concentrations. An automated Rudolph Research thin-film null ellipsometer (43603-20E) was used to measure the

adsorption of PVNP on silica and cellulose surfaces. Details of the instrument set up can be found in ref.[35] Ellipsometry measures the change of polarized light in terms of the relative phase shift, Δ, and the relative amplitude change, Ψ, upon reflection against the interface. From these parameters, the optical properties of the substrate, as well as the refractive index, n_s, and the thickness of the adsorbed films, d_f, can be determined.[35,36] The adsorbed amount (Γ) was calculated using the de Feijter's approach.[37]

$$\Gamma = d_f(n_s - n_0)\left(\frac{dn}{dc}\right)^{-1} \tag{1}$$

where n_0 is the refractive index of the salt solution, while dn/dc is the refractive index increment of the adsorbed molecules. The refractive index increment measurements are provided in the Supporting Information of our previous work.[29] The optical models employed to determine the silica substrate and adsorbed layer properties, were based on three (with polymer) or four (without polymer) layers: Si-SiO_2-Bulk or Si-SiO_2-Polymer film-Bulk. The optical properties and thickness of the SiO_2 layer can be determined by measuring the Ψ and Δ values in two different media, air and water. The formation of a polyelectrolyte layer changes Ψ and Δ, and this change can be used to estimate the refractive index, n_s, and the thickness, d_f, of the film, from which the adsorbed amount can be calculated.

A two (with polymer) or three (without polymer layer model, Substrate-Bulk, or Substrate-Polymer film-Bulk, was used for cellulose surfaces, under the assumption that the optical properties of the cellulose layer remains unchanged upon polymer adsorption. In this simple model, the optical properties of the substrate were only measured in liquid media. Therefore, n_s and d_f cannot be resolved independently, but the adsorbed amount can still be calculated accurately.

Theoretical considerations

We shall test two slightly different models for the predictions of polymer adsorption. They do, however, share a common general treatment of polymer configurations, which are handled by

classical density functional theory. We shall therefore first briefly recapitulate this part, and then describe the way in which our two models differ.

Classical density functional theory

Here, we give a brief summary of Woodward's classical density functional theory[38] (DFT). Subsequent work has provided important extensions to this theory,[39,40] some of which will be utilized in this work.

An illustration of the way in which the polymers are modelled, is shown in Figure 2. As in parts of ref.,[29] we utilize a "comb-like" structure, where each monomer is built up by four beads that dangle out from a joining backbone. The end bead of each "comb" carries a unit (positive) charge.

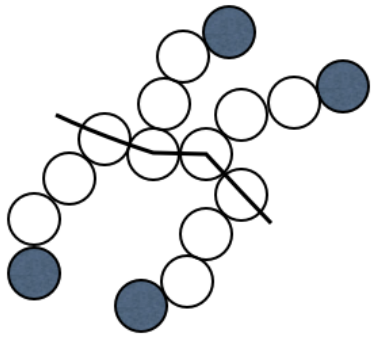

Figure 2: An illustration of our polymer model. Each monomer is represented by four connected hard-sphere beads. The shaded spheres (at the end of each side chain) carry a unit charge, i.e., the charge of the monomer.

We will only treat monodisperse polymers, each of which are composed of q connected beads. We let $N(\mathbf{R})d\mathbf{R}$ denote a density distribution of polymers with configuration $\mathbf{R} = \mathbf{r}_1, \mathbf{r}_2, ..., \mathbf{r}_q$, where $\mathbf{r}_i$ is the coordinate of bead i. The beads are joined together by an orientationally flexible bond potential V_b, chosen to ensure a constant bond length d: $e^{-\beta V_b(\mathbf{R})} \propto \prod \delta(|\mathbf{r}_{i+1} - \mathbf{r}_i| - d)$, where $\delta(x)$ is the Dirac delta function, while the inverse thermal energy is denoted by $\beta = 1/(kT)$. The beads are themselves modelled as hard spheres, of diameter d, i.e. the connected beads form a pearl-necklace structure (perhaps better described as a comb-like pearl necklace). The grand potential of the polymer solution, in the presence of an external field, $V_{ex}(\mathbf{r})$ (our model of the

silica surface), can be written as:[38]

$$\Omega = \mathscr{F}^{(id)} + \mathscr{F}_{HS}^{(ex)}[n_m(\mathbf{r})] + \mathscr{U}[n_c(\mathbf{r})] - \mu_p \int N(\mathbf{R}) d\mathbf{R} \tag{2}$$

where $\mathscr{F}_p^{id}$ denote the *exact* free energy functional for ideal chains (with point-like monomers):

$$\beta \mathscr{F}_p^{(id)} = \int N(\mathbf{R}) \left(\ln[N(\mathbf{R})] - 1\right) d\mathbf{R} + \beta \int N(\mathbf{R}) V_b(\mathbf{R}) d\mathbf{R} + \beta \int n_m(\mathbf{r}) V_{ex}(\mathbf{r}) d\mathbf{r} \tag{3}$$

Here, $n_m(\mathbf{r})$ is the bead density, while we let $n_c(\mathbf{r})$ denote the density of *charged* beads. Inter-particle interactions can only be approximately accounted for, and $\mathscr{F}_{HS}{}^{(ex)}[n_m(\mathbf{r})]$ denotes the part of the functional that handles excluded volume effects. We have utilized the "Generalized Flory-Dimer" formulation, introduced by Hall and co-workers.[41] This equation of state can, upon integration, be formulated as a free energy functional, as described elsewhere.[39] The charged beads also interact via a screened Coulomb potential, and these interactions are contained in the energy functional term, $\mathscr{U}[n_c(\mathbf{r})]$. Equilibrium with a bulk solution is ensured by the polymer chemical potential, μ_p, which effectively acts as a Lagrange multiplier.

As already mentioned, we assume that the Coulomb interactions between charged species are screened by (implicit) monovalent salt, as quantified by the Debye-Hückel screening length, κ^{-1}: $\kappa^2 = 2\frac{\beta c_S e^2}{\varepsilon_r \varepsilon_0}$. Here, c_S is the bulk concentration of monovalent simple salt, e is the elementary charge, ε_0 is the dielectric permittivity of vacuum, and $\varepsilon_r = 78.3$ is the (uniform) dielectric constant of the implicit aqueous solvent. Electrostatic interactions between charged beads, u_{cc}, are thus approximated by:

$$\beta u_{cc} = \frac{l_B e^{-\kappa r}}{r} \tag{4}$$

where r is the bead-bead separation, while the Bjerrum length, l_B, at room temperature and in an aqueous environment, is about $0.716nm$.

The importance of including ion correlations, albeit in an approximate manner, has been demonstrated in several previous works.[28,29,42] Here we shall use the approximations suggested by Fors-

man and Nordholm.[42] Consider a system with a pairwise additive interaction potential $\phi(r)$. The mean-field interaction energy per particle, $e_p^{(mf)}(\mathbf{r})$, can then be written as:

$$e_p^{(mf)}(\mathbf{r}) = \frac{1}{2}\int n_c(\mathbf{r}')\phi(|\mathbf{r}-\mathbf{r}'|)d\mathbf{r}' \tag{5}$$

This expression includes a spurious self-interaction, which can be corrected for in various ways. Following earlier work, we introduce a "soft correlation hole", and assume that the radial distribution function, $g(r)$, decays exponentially:

$$g(r) = 1 - e^{-\lambda r} \tag{6}$$

Here, λ is chosen such that one particle is excluded. Assuming λ to be position-independent, and determined by the bulk conditions, we obtain a simple analytic formula:

$$\lambda = (8\pi n_b)^{1/3} \tag{7}$$

where n_b in our case is the bulk concentration of *charged* beads, which in our case equals the bulk concentration of monomers [1]. We thus arrive at the following expression for $\mathscr{U}$: of the functional, $\mathscr{U}$, as:

$$\beta\mathscr{U} = \frac{l_B}{2}\int n_c(\mathbf{r})\int n_c(\mathbf{r}')(1-e^{-\lambda(|\mathbf{r}-\mathbf{r}'|)})\frac{e^{-\kappa(|\mathbf{r}-\mathbf{r}'|)}}{|\mathbf{r}-\mathbf{r}'|}d\mathbf{r}'d\mathbf{r} \tag{8}$$

The bulk monomer (or charged bead) concentration is given by the experimental conditions, i.e. n_b =0.2 mM.

Non-electrostatic surface interaction

The substrate silica surface, i.e. V_{ex}, is modelled as an infinitely large flat wall, extending indefinitely in the x,y directions. Integrating across the x,y dimensions, in a mean-field manner, allows us to express our functional in terms of density distributions along the z axis.

[1] Note that each monomer is composed of several beads, one of which carries a unit charge.

$V_{ex}(z)$ can be written as a sum of an electrostatic ($w_{el}(z)$) and a non-electrostatic ($w_s(z)$) part: $V_{ex}(z) = w_{el}(z) + w_s(z)$. The non-electrostatic part acts equally on *all* beads, i.e. charged as well as neutral, and is given by:

$$\beta w_s(z) = \left(\frac{d_w}{z}\right)^6 - \gamma\left(\frac{d_w}{z}\right)^3 \tag{9}$$

where d_w determines the range of the potential, while γ regulates the non-electrostatic affinity.

Adsorption

Having established an equilibrium bead distribution, $n_m(z)$, we obtain the net absorption, Γ, as:

$$\Gamma = \int_0^\infty (n_m(z) - n_m(bulk))dz \tag{10}$$

where $n_m(bulk)$ is the bulk concentration of beads. A drawback of the experimental technique is that the obtained information does not allow elaborate models of the density profile. Instead, a simple slab model is adopted, i.e., a step-wise profile (or a very limited set of step-wise profiles) is assumed. Reported adsorption measurement furthermore relies upon an extrapolation (sometimes rather drastic) of bulk refractive index data. Another challenge, when comparing experiments and theoretical predictions, is surface roughness, which is absent in our theoretical modelling. Cellulose surfaces are further complicated by the fact that they are at least to some extent porous. This will be further discussed below. As the monomer molecular weight is almost identical for the two polymers we have investigated, we shall adopt a common monomer+chloride (counterion) weight of 160 g/mol.

Models

We shall now describe our two different models. They primarily differ in the way that the electrostatic interactions with the silica surface are modelled. However, they also differ in the way in which we distinguish between PVNP and PDADMAC. In model I, which is almost identical

to that used in our previous work,[29] the hard-sphere diameter "d", is the same for the PVNP and PDADMAC models, but the strength (γ) of the non-electrostatic adsorption (w_s) differ. In model II, we retain the latter, but allow d to vary between the two monomeric types, assuming that PVNP monomers effectively occupy less volume (in a potential of mean force sense) than PDADMAC monomers. These considerations, as well as our two different descriptions of surface electrostatics, will be further detailed below.

Model I

Since this model is essentially identical to the one used in ref.,[29] we will only provide a rather condensed description. In that work, we chose surface charge densities, according to titration values reported by Bolt[43] on silica particles. Unfortunately, we use a different kind of silica, the titration properties of which have not been accurately measured. Horiuchi *et al.*[44] did investigate the charge concentration on the surface of silica wafers, but only at a salt concentration of 50 mM. The surface charge density they measured at pH 9, essentially coincides with the corresponding value reported by Bolt, albeit at a salt concentration of just 10 mM. This implies that our silica might typically be less charged than the silica particles investigated by Bolt. Keeping this in mind, we shall nevertheless allow ourselves to be guided by titration results on silica particles. However, in contrast to our previous work,[29] we will assume that the surface is fully charged at all salt concentrations. This is motivated by our results using a titrating surface below (model II), and also by experimental results by Samoshina *et al.*[15] These results suggest that, in the presence of a highly charged polymer, a silica surface will become fully charged irrespective of the salt concentration (at pH 9). Still, as we will show below, the modification of our previous model, in which the charge density increased with salt, does not lead to a substantial change of the predictions, provided that we are allowed to make a similar modification of the non-electrostatic potential (γ). Recall that this quantity presumably reflects solvent-induced potential of mean forces, quite possibly hydrophobic interactions. These are obviously poorly established in our coarse-grained model, which emphasizes that γ is best regarded as a fitting parameter. In fact, in model II, this is not even changed

between our models of PVNP and PDADMAC. Kobayashi *et al.*[45] arrived at a maximum surface absolute charge density of $|\sigma_s| = 8^{-1}\ e/nm^2$, where e is the elementary charge for silica particles, which is commensurate with the titration curves of Bolt. Hence, we shall set this as our fixed value, in model I. Furthermore, in model I, the electrostatic contribution, which of course only acts on the charged beads, is taken from the standard Guy-Chapman model:

$$\beta w_{el} = 2\ln\left[\frac{1+\Gamma_0 e^{-\kappa z}}{1-\Gamma_0 e^{-\kappa z}}\right] \tag{11}$$

where

$$\Gamma_0 = tanh\left[\frac{\beta w_0}{4}\right] \tag{12}$$

with

$$\beta w_0 = 2sinh^{-1}\left[\frac{\sigma_s}{\sqrt{8kTc_s\varepsilon_0\varepsilon_r}}\right] \tag{13}$$

PVNP and PDADMAC are discriminated by the value of the non-electrostatic surface affinity, γ. The wall potential range parameter d_w is here set equal to the bead diameter d, which is common to both polymer models. Specifically, we have set $d_w = d = 0.25nm$, which is identical to the value used in ref.[29] Adjusting γ such that the slope of the adsorption curves for long-chain PVNP and PDADMAC are reproduced (as in ref.[29]) leads to $\gamma = 2$ and $\gamma = \sqrt{1.6}$ for PVNP and PDADMAC, respectively. This leads to minimum non-electrostatic potential values of $\beta w_{min} = -1$ and -0.4, respectively. In our predictions for short chain PVNP, we have naturally adopted the same parameters as for the higher molecular weight PVNP.

Model II

In this model, we will explicitly consider that the silica surface titrates in the presence of salt and polyelectrolyte. While it is true that the precise titration properties are only determined with low accuracy, we do have some reasonable estimates, since these properties hardly are completely different from the surfaces of silica particles. Given that electrostatic interactions between charged

beads are described by screened Coulomb interactions, we can only arrive at a consistent treatment if the surface charges are handled in an analogous manner. In other words, we will here assume that charged surface sites interacts with monomers as well as other surface sites via a screened Coulomb potential:

$$\beta u_{s\alpha} = -\frac{z_\alpha l_B e^{-\kappa r}}{r} \tag{14}$$

where "s" stands for surface site, while $z_c = 1$ and $z_s = -1$ is the valency of charged beads and surface sites, respectively. Upon integration along x, y dimensions parallel with the surfaces, we arrive at the following expression for the mean-field interaction energy, e_s^{mf} for an adsorbed hydrogen ion:

$$\beta e_p^{mf} = 2\pi\kappa^{-1} l_B \left(\frac{1}{2}\Gamma_s(\theta - 1) + \int_0^\infty n_c(z) e^{-\kappa z} dz \right) \tag{15}$$

where θ is the fraction of sites that are occupied by hydrogen ions, while Γ_s is total density of surface sites $\Gamma_s \equiv |\sigma_s|/e$. Note that $|\sigma_s|$, should be regarded as an *effective* maximum absolute surface charge density, as measured at the Helmholtz plane. The mean-field interaction energy per unit area, u_s, for adsorbed hydrogen ions, is:

$$\beta u_s = 2\pi\kappa^{-1} l_B \Gamma_s \left(\frac{1}{2}\Gamma_s(\theta - 1)^2 + (\theta - 1) \int_0^\infty n_c(z) e^{-\kappa z} dz \right) \tag{16}$$

the derivative of which provides the interaction contribution, μ_u, to the chemical potential:

$$\beta \mu_u = 2\pi\kappa^{-1} l_B \left(\Gamma_s(\theta - 1) + \int_0^\infty n_c(z) e^{-\kappa z} dz \right) \tag{17}$$

We furthermore define K as an effective intrinsic association constant:[46]

$$K = \frac{\theta}{(1 - \theta) c_H(0)} \tag{18}$$

where $c_H(0)$ is the proton concentration at the Helmholtz plane. If we approximate the activity by the bulk concentration of hydrogen ions, $[H^+]_b$, equilibrium between bulk and surface leads us to

the following relation for θ:

$$\theta = [H]_b^+ K(1-\theta)e^{-\beta\mu_u} \tag{19}$$

to be iterated until self-consistence, for the given monomer density profile.

Titrations in a simple electrolyte

We will have to make some inevitable assumptions about the parameters controlling the titration. We note that $e\Gamma_s$ is expected to be smaller than the maximum absolute value of the charge density at the bare surface, $|\sigma_s|$. Recalling that an experimentally estimated value of the latter is $8^{-1}\ e/nm^2$,[45] we thus expect $e\Gamma_s$ to have a lower value (at the Helmholtz plane), with the caveat that our silica surface differ somewhat from the ones on silica particles. In other words, the maximum *effective* surface charge density is less that the maximum *bare* surface charge density. More specifically, we have assumed that $e\Gamma_s = 15^{-1}\ e/nm^2$. While this is a crude estimate, it is a reasonable one, and it also leads to realistic predictions, as we shall see. The electrostatic properties of our model surface also depend upon the effective association constant, K. In Figure 3, we see how the titration curves respond to changes of the value assigned to K, at various concentration of simple salt (no polyelectrolyte). We have then defined a reference value of K, as: $K_{ref} = 10^6 nm^3$.

According to the titration curves established by Bolt,[43] the silica surface has reached about half its maximum absolute value at pH 9, when the salt concentration is 10 mM. On the other hand, adding salt, to 1000 mM, will see the surface almost fully charged, at this pH. Comparing with the results presented in Figure 3, this suggests that $K \approx 10 - 100K_{ref}$ are reasonable estimates. This is of course very crude, but fortunately (see below) our predictions of polyelectrolyte adsorption are quite insensitive to the choice of K.

Discriminating between polyelectrolytes

In model I, we will discriminate between PVNP and PDADMAC by the non-electrostatic potential, i.e. the value of γ. The precise origin of this is not specified in our coarse-grained model, but it

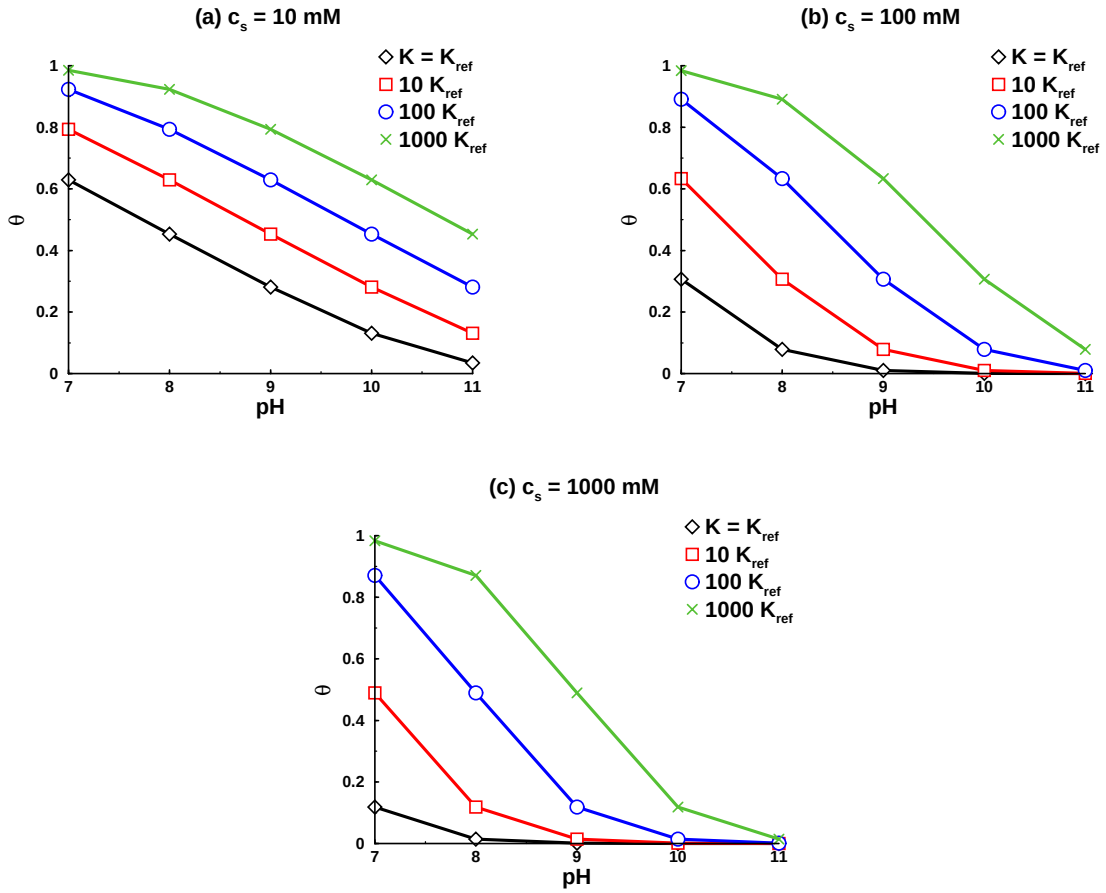

Figure 3: Titration curves, established for various choices of the apparent association constant, K, at different salt concentrations. These were obtained in the absence of polyelectrolyte. $K_{ref} = 10^6 nm^3$.
(a) Surface protonation fraction at $c_s = 10mM$
(b) Surface protonation fraction at $c_s = 100mM$
(c) Surface protonation fraction at $c_s = 1000mM$

could for instance imply that one monomer type is pushed more strongly to the surface than the other, due to a difference in hydrophobicity. We could use a similar approach here, but it might be relevant to illustrate that the polyelectrolytes in principle can be discriminated in other ways. In contrast to model I, we will here assume that the beads experience an *identical* non-electrostatic surface potential. The polymers are instead identified by the volume excluded by the beads that build up the monomers, i.e. by the value of d. Specifically, we shall set $d = 0.25nm$ for the beads of "PDADMAC", whereas the corresponding value of "PVNP" is $d = 0.2nm$ (the bond length is in both cases equal to the bead diameter). This could either be interpreted as PVNP monomers being

able to pack more efficiently than those of PDADMAC, or as water being better able to solvate the monomers of PDADMAC. The latter interpretation would be motivated by an effectively more repulsive potential of mean force between the building blocks of a more hydrophilic polymer. The common non-electrostatic surface potential is characterized by $d_w = 0.30nm$, and a minimum value of $\beta w_{min} = -0.6$ ($\gamma = \sqrt{2}.4$). In an analogous fashion to model I, the value of d for the respective monomer beads (belonging to "PVNP" and "PDADMAC") were adjusted to roughly match the slope of the adsorption curves at high salt, in each case. This value is then retained for the predictions of the adsorption of short chain PVNP.

Comments on the modelling

Our models are inevitably based on some assumptions, but we have here, and earlier works, spent efforts on testing and validating some of them. In ref.,[28] DFT predictions on polyelectrolyte adsorption at charged surfaces was tested against simulations, on identical models. Responses to changes of polymer length, as well as the addition of salt was investigated, at flat surfaces as well as at spherical particles. DFT was shown to be satisfactorily accurate, provided that a treatent (approximate) of electrostatic correlations was included. In ref.,[42] interactions between charged particles, in the presence of polyelectrolytes and symmetric or asymmetric salts, were studied. In the same study, comparisons between models using an explicit (full Coulomb) or implicit (screened Coulomb) representation of simple monovalent ions, were also made. The screened Coulomb + DFT approach provided remarkably accurate predictions. In ref.,[29] we utilized DFT to investigate predictions on the adsorbed amount of polyelectrolytes at a charged surface. Test were made to verify that the predictions were robust, with respect to polymer architecture, chain stiffness, excluded volume treatment, and polydispersity. The predictions were found to be robust, although the results were somewhat sensitive to polydispersity, when the degree of polymerization was small.

Results

Silica surfaces

Examples of how the experimentally measured adsorption of short chain PVNP on silica substrate varies with time are provided in Figure 4. The complete set of measurements is provided in the Supporting Information. The adsorption curves are reproducible to within about $\pm 5\%$ of the determined adsorbed amount, and under all investigated conditions, they approached a plateau value.

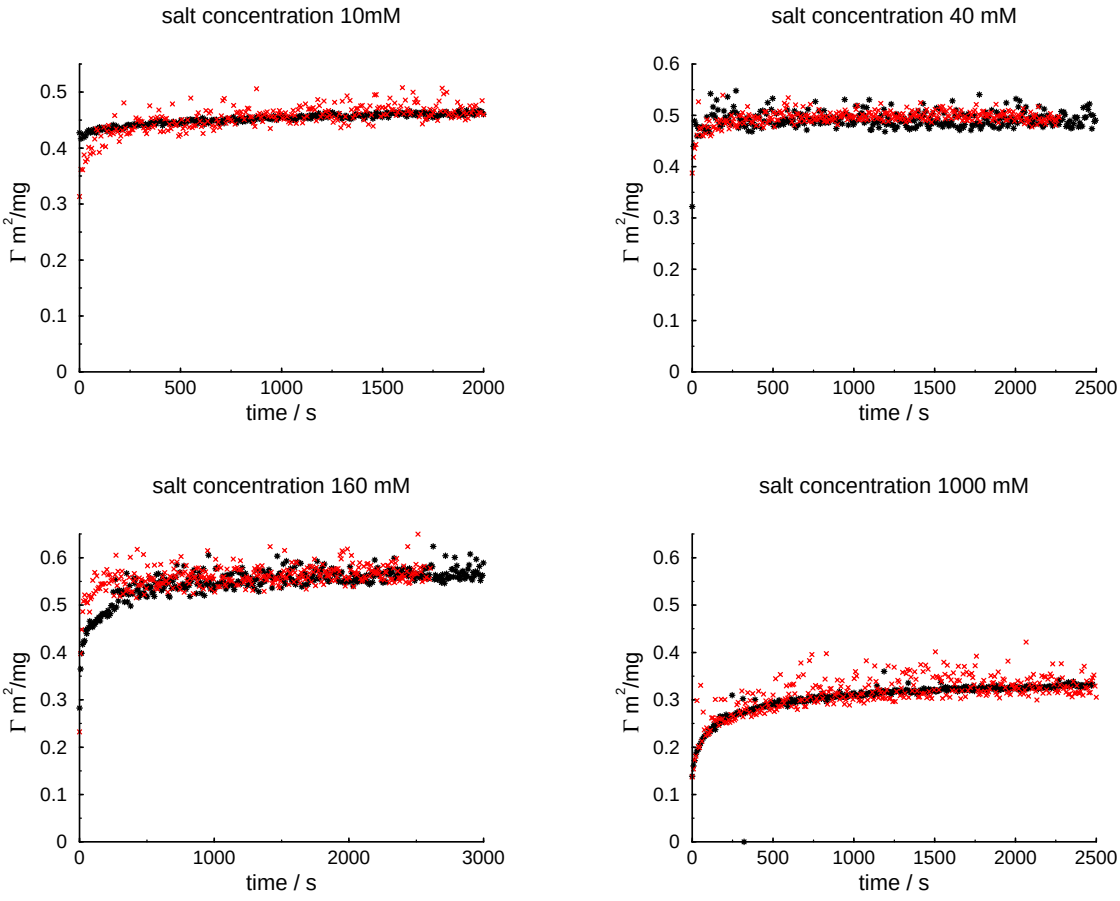

Figure 4: Adsorbed amount of short chain PVNP on silica surface as a function of time at different NaCl concentration (10mM, 40mM, 160mM, 1000mM) at pH 9. Red and black curves indicate two independent measurements.

Comparisons between theoretical predictions and experimental measurements are summarized in Figure 5 (utilizing Model I) and Figure 6 (utilizing Model II). Experimental adsorption results

of long chain PVNP and PDADMAC have been published in our previous work,[29] and are reproduced here, for comparisons with our theoretical predictions. The polyelectrolyte adsorption initially increase with salt concentration, but reaches a maximum, followed by a gradual decrease of the adsorbed amount. The maximum most likely originates from a balance between competing electrostatic interactions: while the polyions are attracted to the oppositely charged surface, a stronger adsorption also results in an increased repulsion between like-charged species within the adsorbed layer. All these electrostatic interactions are screened as salt is added, resulting in the net outcome of a maximum adsorption at a certain salt level. At least for PVNP, there seems to be a limiting plateau value (for long as well as short chains) at high levels of salt, possibly due to hydrophobic interations. All the theoretical models are able to reproduce the main trend of the experimental adsorption curves. This indicates the that our coarse-grained models capture the main physics of adsorption in these systems. On the other hand, the difference between our models also highlights that our ability to identify details of the molecular mechanisms underlying the differences between PVNP and PDADMAC is limited. In our previous work,[29] we demonstrated that polydispersity effects are pronounced for short chains, but nearly negligible for high degrees of polymerization. The underlying reason is that polymer length effects are substantial for short chains, but that this dependence almost vanishes as the polymer length increase. The polydispersity reported from the manufacturer is actually rather low (1.15) for the short PVNP, but there is reason to believe that the polyelectrolyte adsorption will be dominated by the longer chains in this sample, i.e. even though the average polymer length is about 18 (M_w value), the adsorption is most likely akin to a monodipserse sample with a somewhat higher degree of polymerization. In Figure 6, we illustrate these effects by including predictions from monodisperse chains with a slightly higher degree of polymerization (20). These are given by the dashed orange curve. For polymers with a high molecular weight, on the other hand, polydispersity effects are predicted to be small (see ref.[29] for details).

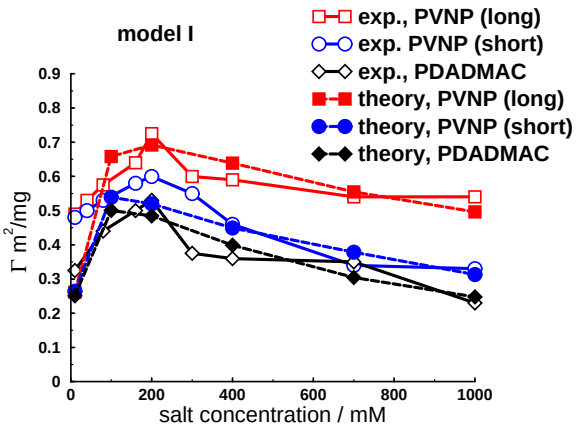

Figure 5: Experimental measurements and theoretical predictions (Model I) of adsorbed amount for different types of polyelectrolytes on silica, as a function of salt concentration at pH 9. Experimental data for PDADMAC and long chain PVNP are taken from ref.[29]

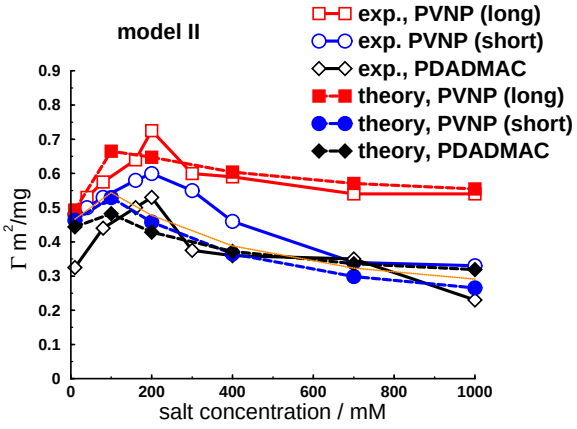

Figure 6: Experimental measurements and theoretical predictions (Model II) of adsorbed amount for different types of polyelectrolytes on silica, as a function of salt concentration at pH 9. The thin dashed line shows short chain predictions for monodisperse 20-mers, rather than our "standard" 18-mers (the latter being based on the manufacturer reported value for M_w).

In model II, the surfaces are allowed to titrate. As mentioned earlier, we have set $K = 10K_{ref}$, although we did point out that this is only a crude estimate, obtained from consideration of how a surface titrates in the presence of monovalent simple samlt. Fortunately, our polyelectrolyte adsorption predictions are quite insensitive to the choice of K. This is illustrated in Figure 7, where predicted results for a wide range of chosen K values are shown. We only see a significant change when K becomes about three orders of magnitude larger than K_{ref}, i.e. about two orders

of magnitude larger than the value we have chosen to use. However, upon comparing with the titration obtained in the presence of the pure monovalent salt, cf. Figure 3, we note that such high values of K are unrealistic, and do not mimic the properties of silica.

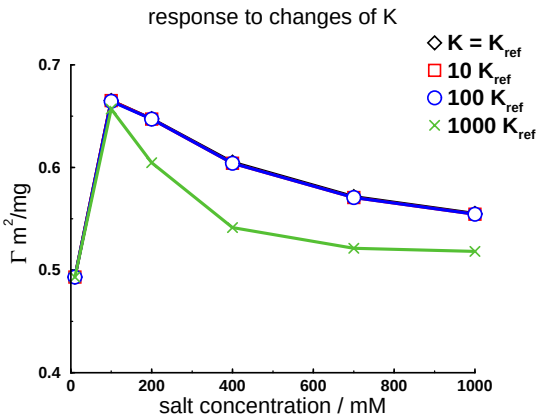

Figure 7: Test of how model II predictions responds to changes of the chosen effective association constant, K. Here, we display results for our model of long chain PVNP, but the response is similar for our models of short chain PVNP and PDADMAC (not shown).

The reason why the polymer adsorption predictions are so insensitive to changes of K is that, for any realistic choice, the surface becomes almost fully charged in the presence of oppositely charged polyions, irrespective of the ionic strength. This is expected, and also motivates our choice of a fully charged surface at all salt concentrations, using model I.

Cellulose surfaces

Examples of how the measured adsorption of long chain PVNP on cellulose surfaces varies with time are provided in Figure 8. The complete set of measurements is provided in the Supporting Information. We were able to get reproducible and stable adsorption values, at all investigated salt concentrations.

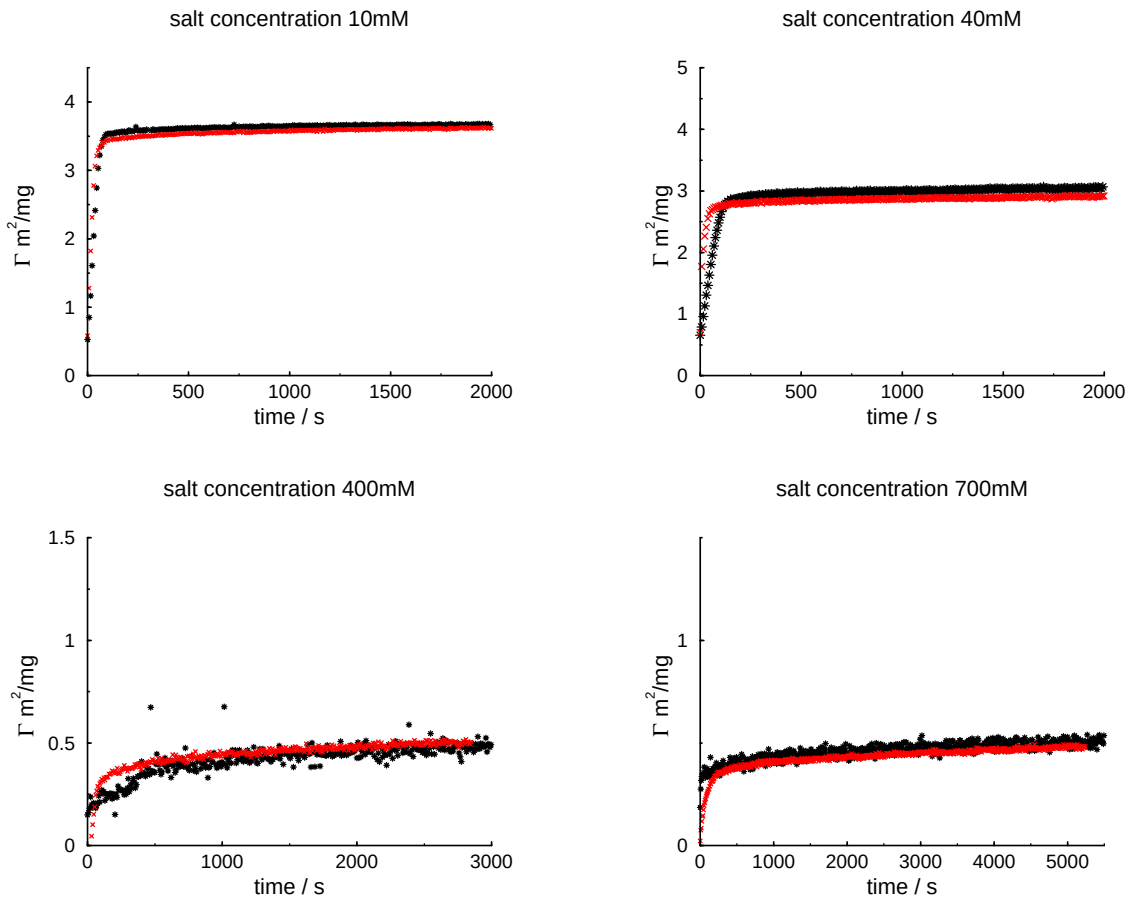

Figure 8: Adsorbed amount of long chain PVNP on cellulose surface as a function of time at different NaCl concentration (10mM, 40mM, 400mM, 700mM) at pH 9. Red and black curves indicate two independent measurements.

The amount plateau value of the adsorbed amount for long chain PVNP on cellulose surfaces, varies with the salt concentration. This is illustrated in Figure 9. We note that the adsorption of long chain PVNP to cellulose is considerably higher than on silica surfaces. This may be due to the cellulose surface being rougher than silica, i.e. that the actual surface area for the cellulose substrate is substantially larger than the projected one.

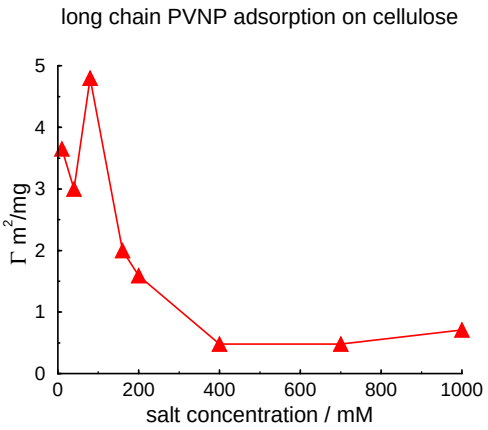

Figure 9: Adsorbed amount of long chain PVNP on cellulose surface as a function of different NaCl concentration at pH 9.

In this case, the adsorbed amount at 10 mM salt seems to be slightly *larger* than at 40 mM, followed by an increase at 100 mM. The underlying reason for the initial dip of the adsorbed amount is unclear to us, but these effects are possibly related to cellulose swelling, which might generate a salt dependence of the effective available surface area. Still, it should be emphasized that the observed difference in adsorbed amount between 10 mM and 40 mM salt is quite small.

Unfortunately, despite considerable efforts, we have been unable to obtain converged values for the adsorbed amount of short chain PVNP on cellulose. Specifically, for some salt concentrations (particularly at low values), the adsorption curve is monotonically increasing, seemingly without reaching a plateau value, despite rather long measuring times. This may indicate that the short chain PVNP is able to partly penetrate into cellulose surfaces, even at low salt. This diffusion process may be quite slow, which could explain the observed slow kinetics. In other words, small polyions, that are slowly penetrating the cellulose network, would be replaced at the outer surface by adsorption from the bulk, with the former (slow) process determining the overall kinetics. This mechanism could also explain why the adsorption level at low salt seems to be *higher* for short chains (with the caveat of a very slow equilibration process), assuming that the long polymers are too large to enter the cellulose matrix. Given our experimental observations, we have refrained from any theoretical modelling of polyelectrolyte adsorption to cellulose surfaces. The whole set of

short chain PVNP on cellulose surfaces measurements is provided in the Supporting Information.

Conclusions

In summary, we have established that the adsorbed amount of highly charged polymers at an oppositely charged (and impenetrable) silica surface, drop when the chains become short enough. This is corroborated by theoretical predictions, where the latter are robust in the sense that they are insensitive to changes of model details. At a cellulose surface, the situation is more complex, and we have not always been able to establish plateau values of the adsorbed amount for short polymers. In other words, the adsorption process seems to be very slow, in this case. We speculate that the strong adsorption found for short polyions at low salt concentrations, as well as the long equilibration times, originate from a slow penetration into the cellulose matrix - a process that seems to be negligible for our long polyions (at low salt). In all cases where we have been able to determine an equilibrium adsorbed amount, the adsorption displays a maximum for some threshold salt concentration.

Acknowledgments

We acknowledge the Swedish Research Council for financial support.

References

1. Lindquist, G. M.; Stratton, R. A. The role of polyelectrolyte charge density and molecular weight on the adsorption and flocculation of colloidal silica with polyethylenimine. *J. Coll. Int. Sci.* **1976**, *55*, 45.

2. Papenhuizen, J.; van der Schee, H. A.; Fleer, G. Polyelectrolyte adsorption: I. A new lattice theory. *J. Coll. Int. Sci.* **1985**, 540.

3. Papenhuizen, J.; Fleer, B. H., G.and Bijsterbosch Polyelectrolyte adsorption: II. Comparison of experimental results for polystyrene sulfonate, adsorbed on polyoxymethylene crystals, with theoretical predictions. *J. Coll. Int. Sci.* **1985**, 553.

4. Muthukumar, M. Adsorption of a polyelectrolyte chain to a charged surface. *J. Chem. Phys.* **1987**, *86*, 7230–7235.

5. van de Steeg, H. G. M.; Cohen Stuart, M. A.; de Keizer, A.; Bijsterbosch, B. H. Polyelectrolyte adsorption: a subtle balance of forces. *Langmuir* **1992**, *8*, 2538.

6. Nordholm, S.; Rasmusson, M.; Wall, S. Simple analysis of the electrostatic screening mechanism in flocculation. *Nordic Pulp and Paper Res. J.* **1993**, *8*, 160.

7. Shubin, V.; Linse, P. Effect of Electrolytes on Adsorption of Cationic Polyacrylamide on Silica: Ellipsometric Study and Theoretical Modeling. *J. Phys. Chem.* **1995**, *99*, 1285.

8. Dobrynin, A. V.; Deshkovski, A.; Rubinstein, M. Theory of polyelectrolytes in solutions and at surfaces. *Macromol.* **2001**, *34*, 3421.

9. Kong, C. Y.; Muthukumar, M. Monte Carlo study of adsorption of a polyelectrolyte onto charged surfaces. *J. Chem. Phys.* **1998**, *109*, 1522.

10. Rehmet, R.; Killmann, E. Adsorption of cationic poly(diallyl-dimethyl-ammoniumchloride), poly(diallyl-dimethyl-ammoniumchloride-co-N-methyl-N-vinylactamide) and poly(N-methyl-N-vinyl-acetamide) on polystyrene latex. *Colloid Surface* **1999**, *149*, 323–328.

11. Meszaros, R.; Thompson, L.; Bos, M.; de Groot, P. Adsorption and Electrokinetic Properties of Polyethylenimine on Silica Surfaces. *Langmuir* **2002**, *18*, 6164.

12. Hansupalak, N.; Santore, M. M. Sharp Polyelectrolyte Adsorption Cutoff Induced by a Monovalent Salt. *Langmuir* **2003**, *19*.

13. Shafir, A.; Andelman, D.; Netz, R. Adsorption and depletion of polyelectrolytes from charged surfaces. *J. Chem. Phys* **2003**, *119*, 2355.

14. Netz, R.; Andelman, D. Neutral and charged polymers at interfaces. *Physics Reports* **2003**, *380*, 1.

15. Samoshina, Y.; Nylander, T.; Shubin, V.; Bauer, R.; Eskilsson, K. Equilibrium Aspects of Polycation Adsorption on Silica Surface.âĂL' How the Adsorbed Layer Responds to Changes in Bulk Solutio. *Langmuir* **2005**, *21*, 5872–5881, PMID: 15952836.

16. Ondaral, S.; Wågberg, L.; Enarsson, L.-E. The adsorption of hyperbranched polymers on silicon oxide surfaces. *J. of Coll. Int. Sci.* **2006**, *301*, 32 – 39.

17. Carillo, J.-M. Y.; Dobrynin, A. V. Molecular Dynamics Simulations of Polyelectrolyte Adsorption. *Langmuir* **2007**, *23*, 2482.

18. Popa, I.; Cahill, B. P.; Maroni, P.; Papastavrou, G.; Borkovec, M. Thin adsorbed films of a strong cationic polyelectrolyte on silica substrates. *J. Coll. Int. Sci.* **2007**, *309*, 28 – 35, Matijevic Festschrift.

19. Enarsson, L.-E.; Wågberg, L. Adsorption Kinetics of Cationic Polyelectrolytes Studied with Stagnation Point Adsorption Reflectometry and Quart z Crystal Microgravimetry. *Langmuir* **2008**, *24*, 7329–7337, PMID: 18553950.

20. Enarsson, L.-E.; Wågberg, L. Polyelectrolyte Adsorption on Thin Cellulose Films Studied with Reflectometry and Quartz Crystal Microgravimetry with Dissipation. *Biomacromol.* **2009**, *10*, 134–141.

21. Saarinen, T.; Österberg, M.; Laine, J. Properties of Cationic Polyelectrolyte Layers Adsorbed on Silica and Cellulose Surfaces Studied by QCM-D-Effect of Polyelectrolyte Charge Density and Molecular Weight. *J. Coll. Disp. Sci.* **2009**, *30*, 969.

22. Guzm*á*n, E.; Ortega, F.; Baghdadli, N.; Luengo, G. S.; Rubio, R. G. Effect of the molecular structure on the adsorption of conditioning polyelectrolytes on solid substrates. *Colloid Surface* **2011**, *375*, 209 – 218.

23. Hierrezuelo, J.; Szilagyi, I.; Vaccaro, A.; Borkovec, M. Probing Nanometer-Thick Polyelectrolyte Layers Adsorbed on Oppositely Charged Particles by Dynamic Light Scattering. *Macromol.* **2010**, *43*, 9108.

24. Jiang, M.; Popa, I.; Maroni, P.; Borkovec, M. Adsorption of poly(l-lysine) on silica probed by optical reflectometry. *Colloid Surface* **2010**, *360*, 20 – 25.

25. Seyrek, E.; Hierrezuelo, J.; Sadeghpour, A. J.; Szilagyi, I.; Borkovec, M. Molecular mass dependence of adsorbed amount and hydrodynamic thickness of polyelectrolyte layers. *Phys. Chem. Chem. Phys.* **2011**, *13*, 12716.

26. Turesson, M.; Labbez, C.; Nonat, A. Calcium Mediated Polyelectrolyte Adsorption on Like-Charged Surfaces. *Langmuir* **2011**, *27*, 13572–13581, PMID: 21992756.

27. Guzman, E.; Ortega, F.; Baghdadli, N.; Cazeneuve, C.; Luengo, G. S.; Rubio, R. G. Adsorption of Conditioning Polymers on Solid Substrates with Different Charge Density. *ACS Appl. Mater. Int.* **2011**, *3*, 3181–3188, PMID: 21749104.

28. Forsman, J. Polyelectrolyte Adsorption: Electrostatic Mechanisms and Nonmonotonic Responses to Salt Addition. *Langmuir* **2012**, *28*, 5138.

29. Xie, F.; Nylander, T.; Piculell, L.; Utsel, S.; Wågberg, L.; Åkesson, T.; Forsman, J. Polyelectrolyte Adsorption on Solid Surfaces. Theoretical Predictions and Experimental Measurements. *Langmuir* **2013**, *29*, 12421–12431, PMID: 23980582.

30. Mészáros, R.; Varga, I.; Gilányi, T. The Effect of Salt Concentration on Adsorption of Low-Charge-Density Polyelectrolytes and Interactions between Polyelectrolyte-Coated Surfaces. *Langmuir* **2004**, *20*, 5026–5029.

31. Liufu, S.-C.; Xiao, H.-N.; Li, Y.-P. Adsorption of cationic polyelectrolyte at the solid/liquid interface and dispersion of nanosized silica in water. *J. Coll. Int. Sci.* **2005**, *285*, 33.

32. Rojas, O.; Claesson, P.; Muller, D.; Neuman, R. adsorption of poly(ethyleneimine) on silica surfaces effect of pH on the reversibility of adsorption. *J. Coll. Int. Sci.* **1998**, *205*, 77–88.

33. Fält, S.; Wågberg, L.; Vesterlind, E.-L.; Larsson, P. Model films of cellulose ID – improved preparation method and characterization of the cellulose film. *Cellulose 11*, 151–162.

34. Enarsson, L.-E.; Wågberg, L. Polyelectrolyte Adsorption on Thin Cellulose Films Studied with Reflectometry and Quartz Crystal Microgravimetry with Dissipation. *Biomacromol.* **2009**, *10*, 134–141, PMID: 19053297.

35. Tiberg, F.; Landgren, M. Characterization of thin nonionic surfactant films at the silica/water interface by means of ellipsometry. *Langmuir* **1993**, *9*, 927–932.

36. Azzam, R.; Bashara, N. *Ellipsometry and polarized light*; North-Holland personal library; North-Holland Pub. Co., 1977.

37. De Feijter, J. A.; Benjamins, J.; Veer, F. A. Ellipsometry as a tool to study the adsorption behavior of synthetic and biopolymers at the air water interface. *Biopolymers* **1978**, *17*, 1759–1772.

38. Woodward, C. E. Density functional theory for inhomogeneous polymer solutions. *J. Chem. Phys.* **1991**, *94*, 3183.

39. Woodward, C. E.; Yethiraj, A. Density functional theory for inhomogeneous polymer solutions. *J. Chem. Phys.* **1994**, *100*, 3181.

40. Woodward, C. E.; Forsman, J. Density functional theory for polymer fluids with molecular weight polydispersity. *Phys. Rev. Lett.* **2008**, *100*, 098301.

41. Honnell, K. G.; Hall, C. K. A new equation of state for athermal chains. *J. Chem. Phys.* **1989**, *90*, 1841.

42. Forsman, J.; Nordholm, S. Polyelectrolyte Mediated Interactions in Colloidal Dispersions: Hierarchical Screening, Simulations and a New Classical Density Functional Theory. *Langmuir* **2012**, *28*, 4069.

43. Bolt, G. H. Determination of the charge density of silica sols. *J. Phys. Chem.* **1957**, *61*, 1166.

44. Horiuchi, H.; Nikolov, A.; Wasan, D. T. Calculation of surface potential and surface cherge density by measurement of the three-phase contact angle. *J. Coll. Int. Sci.* **2012**, *385*, 218.

45. Kobayashi, M.; Juillerat, F.; Galletto, P.; Bowen, P.; Borkovec, M. Aggregation and Charging of Colloidal Silica Particles. Effect of Particle Size. *Langmuir* **2005**, *21*, 5761–5769, PMID: 15952820.

46. Gisler, T.; Schulz, S. F.; Borkovec, M.; Sticher, H.; Schurtenberger, P.; Daguano, B.; Klein, R. Understanding colloidal charge renormalization from surface chemistry: Experiment and theory. *J. Chem. Phys.* **1994**, *101*, 9924.